

A measurement of lifetime differences in the neutral *D*-meson system

The FOCUS Collaboration

J.M. Link^a, V.S. Paolone^{a,1}, M. Reyes^{a,2}, P.M. Yager^a,
J.C. Anjos^b, I. Bediaga^b, C. Göbel^{b,3}, J. Magnin^{b,4},
J.M. de Miranda^b, I.M. Pepe^{b,5}, A.C. dos Reis^b,
F.R.A. Simão^b, M.A. Vale^b, S. Carrillo^c, E. Casimiro^{c,6},
H. Mendez^{c,7}, A. Sánchez-Hernández^c, C. Uribe^{c,8},
F. Vazquez^c, L. Cinquini^{d,9}, J.P. Cumalat^d, J.E. Ramirez^d,
B. O'Reilly^d, E.W. Vaandering^d, J.N. Butler^e,
H.W.K. Cheung^e, I. Gaines^e, P.H. Garbincius^e, L.A. Garren^e,
E. Gottschalk^e, S.A. Gourlay^{e,10}, P.H. Kasper^e,
A.E. Kreymer^e, R. Kutschke^e, S. Bianco^f, F.L. Fabbri^f,
S. Sarwar^f, A. Zallo^f, C. Cawfield^g, D.Y. Kim^g, K.S. Park^g,
A. Rahimi^g, J. Wiss^g, R. Gardner^h, Y.S. Chungⁱ, J.S. Kangⁱ,
B.R. Koⁱ, J.W. Kwakⁱ, K.B. Leeⁱ, S.S. Myungⁱ, H. Parkⁱ,
G. Alimonti^j, M. Boschini^j, D. Brambilla^j, B. Caccianiga^j,
A. Calandrino^j, P. D'Angelo^j, M. DiCorato^j, P. Dini^j,
M. Giammarchi^j, P. Inzani^j, F. Leveraro^j, S. Malvezzi^j,
D. Menasce^j, M. Mezzadri^j, L. Milazzo^j, L. Moroni^j,
D. Pedrini^j, F. Prelz^j, M. Rovere^j, A. Sala^j, S. Sala^j,
T.F. Davenport III^k, V. Arena^l, G. Boca^l, G. Bonomi^{l,11},
G. Gianini^l, G. Liguori^l, M. Merlo^l, D. Pantea^{l,12}, S.P. Ratti^l,
C. Riccardi^l, P. Torre^l, L. Viola^l, P. Vitulo^l, H. Hernandez^m,
A.M. Lopez^m, L. Mendez^m, A. Mirles^m, E. Montiel^m,
D. Olaya^{m,13}, J. Quinones^m, C. Rivera^m, Y. Zhang^{m,14},
N. Coptý^{n,15}, M. Purohitⁿ, J.R. Wilsonⁿ, K. Cho^o,
T. Handler^o, D. Engh^p, W.E. Johns^p, M. Hosack^p,
M.S. Nehring^{p,16}, M. Sales^p, P.D. Sheldon^p, K. Stenson^p,
M.S. Webster^p, M. Sheaff^q, Y.J. Kwon^r

^a*University of California, Davis, CA 95616*

^b*Centro Brasileiro de Pesquisas Físicas, Rio de Janeiro, RJ, Brazil*

- ^c*CINVESTAV, 07000 México City, DF, Mexico*
^d*University of Colorado, Boulder, CO 80309*
^e*Fermi National Accelerator Laboratory, Batavia, IL 60510*
^f*Laboratori Nazionali di Frascati dell'INFN, Frascati, Italy, I-00044*
^g*University of Illinois, Urbana-Champaign, IL 61801*
^h*Indiana University, Bloomington, IN 47405*
ⁱ*Korea University, Seoul, Korea 136-701*
^j*INFN and University of Milano, Milano, Italy*
^k*University of North Carolina, Asheville, NC 28804*
^l*Dipartimento di Fisica Nucleare e Teorica and INFN, Pavia, Italy*
^m*University of Puerto Rico, Mayaguez, PR 00681*
ⁿ*University of South Carolina, Columbia, SC 29208*
^o*University of Tennessee, Knoxville, TN 37996*
^p*Vanderbilt University, Nashville, TN 37235*
^q*University of Wisconsin, Madison, WI 53706*
^r*Yonsei University, Seoul, Korea 120-749*

Using a high statistics sample of photoproduced charm particles from the FOCUS experiment at Fermilab, we compare the lifetimes of neutral D mesons decaying via $D^0 \rightarrow K^- \pi^+$ and $K^- K^+$ to measure the lifetime differences between CP even and CP odd final states. These measurements bear on the phenomenology of $D^0 - \bar{D}^0$ mixing. If the $D^0 \rightarrow K^- \pi^+$ is an equal mixture of CP even and CP odd eigenstates, we measure $y_{\text{CP}} = (\Gamma(\text{CP even}) - \Gamma(\text{CP odd})) / (\Gamma(\text{CP even}) + \Gamma(\text{CP odd})) = 0.0342 \pm 0.0139 \pm 0.0074$.

This paper contains a comparison of the lifetimes of a CP even final state, $D^0 \rightarrow K^- K^+$ to the lifetime of a CP mixed decay, $D^0 \rightarrow K^- \pi^+$. The lifetime measurements are made using high signal-to-background D^0 samples consisting of 10 331 decays into $K^- K^+$, and 119 738 decays into $K^- \pi^+$. Throughout this paper, unless stated explicitly, the charge conjugate is implied when a decay mode of a specific charge is stated.

If CP violation in neutral D -meson decays is negligible, the even CP and odd CP combinations of the D^0 and \bar{D}^0 are mass eigenstates with well defined masses and widths. To the extent that $D^0 \leftrightarrow \bar{D}^0$ mixing transitions occur, both the masses and widths of the CP even and odd states may differ. A sizeable mixing contribution through a mass difference may well imply new physics beyond the Standard Model. However, a wide range of predictions on mixing through the width difference appear in the literature [1] which encompass $y_{CP} = (\Gamma(\text{CP even}) - \Gamma(\text{CP odd})) / (\Gamma(\text{CP even}) + \Gamma(\text{CP odd}))$ values of up to several percent. Throughout this paper, we will refer to the width asymmetry between neutral D CP even and odd eigenstates as y_{CP} to differentiate it from the true y mixing parameter which represents the fractional width asymmetry between mass eigenstates and could differ from y_{CP} to the extent that charm decays violate CP symmetry.

Under the assumption that the decay $D^0 \rightarrow K^- \pi^+$ is an equal CP even - odd mixture, the width difference asymmetry (y_{CP}) is related to the measured

¹ Present Address: University of Pittsburgh, Pittsburgh, PA 15260

² Present Address: Instituto de Física y Matemáticas, Universidad Michoacana de San Nicolás de Hidalgo, Morelia, Mich., Mexico 58040

³ Present Address: Instituto de Física, Facultad de Ingeniería, Univ. de la República, Montevideo, Uruguay

⁴ Present Address: Universidad de los Andes, Bogotá, Colombia

⁵ Present Address: Instituto de Física, Universidade Federal da Bahia, Salvador, Brazil

⁶ Present Address: INFN sezione di Milano, Milano, Italy

⁷ Present Address: University of Puerto Rico, Mayaguez, PR 00681

⁸ Present Address: Instituto de Física, Universidad Autónoma de Puebla, Puebla, México

⁹ Present Address: National Center for Atmospheric Research, Boulder, CO

¹⁰ Present Address: Lawrence Berkeley Lab, Berkeley, CA 94720

¹¹ Present Address: Dipartimento di Chimica e Fisica per l'Ingegneria e per i Materiali, Università di Brescia and INFN sezione di Pavia

¹² Present Address: Nat. Inst. of Phys. and Nucl. Eng., Bucharest, Romania

¹³ Present Address: University of Colorado, Boulder, CO 80309

¹⁴ Present Address: Lucent Technology

¹⁵ Present Address: Augusta Technical Inst., Augusta, GA 30906

¹⁶ Present Address: Adams State College, Alamosa, CO 81102

lifetimes via:

$$y_{\text{CP}} = \frac{\Gamma(\text{CP even}) - \Gamma(\text{CP odd})}{\Gamma(\text{CP even}) + \Gamma(\text{CP odd})} = \frac{\tau(D^0 \rightarrow K^- \pi^+)}{\tau(D^0 \rightarrow K^- K^+)} - 1$$

Because $D^0 \rightarrow K^- \pi^+$ is assumed to be a mixed state, a sizeable width difference between the CP even and odd lifetimes and potential interference with doubly-Cabibbo-suppressed decays could, in principle, create a deviation from a pure exponential time evolution. Given the present limits on y [2], this deviation is safely ignored given the scale of our statistical precision. Therefore, we will fit both lifetimes assuming a pure exponential decay.

The data for this paper were collected in the Wideband photoproduction experiment FOCUS during the Fermilab 1996–1997 fixed-target run. FOCUS is a considerably upgraded version of a previous experiment, E687 [3]. In FOCUS, a forward multi-particle spectrometer is used to measure the interactions of high energy photons on a segmented BeO target. We obtained a sample of over 1 million fully reconstructed charm particles in the three decay modes: $D^0 \rightarrow K^- \pi^+$, $K^- \pi^+ \pi^- \pi^+$ and $D^+ \rightarrow K^- \pi^+ \pi^+$. We briefly discuss those aspects of the detector which are particularly relevant for this analysis.

The FOCUS detector is a large aperture, fixed-target spectrometer with excellent vertexing and particle identification. A photon beam is derived from the bremsstrahlung of secondary electrons and positrons with an ≈ 300 GeV endpoint energy produced from the 800 GeV/ c Tevatron proton beam. The charged particles which emerge from the target are tracked by two systems of silicon microvertex detectors. The upstream system, consisting of 4 planes (two views in 2 stations), is interleaved with the experimental target, while the other system lies downstream of the target and consists of twelve planes of microstrips arranged in three views. These detectors provide high resolution separation of primary (production) and secondary (decay) vertices with an average proper time resolution of ≈ 30 fs for 2-track vertices. The momentum of a charged particle is determined by measuring its deflections in two analysis magnets of opposite polarity with five stations of multiwire proportional chambers. Three multicell threshold Čerenkov counters are used to discriminate between electrons, pions, kaons, and protons.

Throughout this analysis we have chosen cuts designed to minimize non-charm backgrounds as well as reflection backgrounds from misidentified charm decays. To minimize potential systematic error, we use cuts and selection techniques which create very little bias in the *reduced* proper time. The reduced proper time is a traditional lifetime variable used in fixed-target experiments which use the detachment between the primary and secondary vertex as their principal tool in reducing non-charm background. The reduced proper time is defined by $t' = (\ell - N\sigma_\ell)/(\beta\gamma c)$ where ℓ is the distance between the primary and secondary vertex, σ_ℓ is the resolution on ℓ , and N is the minimum

“detachment” cut required to tag the charm particle through its lifetime. If absorption and acceptance corrections are small enough that they can be neglected, and if σ_ℓ is independent of ℓ , one can show that the t' distribution for decaying charmed particles, in the absence of mixing effects, will follow an exponential distribution. These assumptions are nearly true in FOCUS.

With a few important differences, many of the basic cuts and analysis algorithms are described in reference [4]. Both states ($D^0 \rightarrow K^-\pi^+$ and K^-K^+) were obtained using a data set which required a minimum detachment of the secondary vertex from the primary vertex¹⁷ of 2.5σ and a high quality secondary vertex with a confidence level exceeding 1%.

To further reduce the background under the signal for $D^0 \rightarrow K^-\pi^+$ and K^+K^- , we required the primary vertex to lie within the boundaries of our segmented target, required the event-by-event proper time resolution to satisfy a cut $\sigma_\ell/(\beta\gamma c) < 60$ fs, and required that the two tracks did not have grossly asymmetric momenta ($|P_1 - P_2|/(P_1 + P_2) < 0.70$). These additional cuts are applied to what we will refer to as the *inclusive* sample. For both decays, we also allow candidates consistent with the decay $D^{*+} \rightarrow D^0\pi^+$ by virtue of having a $D^* - D^0$ mass difference within $3 \text{ MeV}/c^2$ of nominal to be included in the sample without satisfying the proper time resolution and the momentum asymmetry cut. We will refer to this as the *tagged* sample. Both the inclusive and tagged samples were combined to increase statistics for the lifetime analysis of the two charm meson decays. Any overlaps of charm candidates in the combined sample were removed.

Because misidentified Cabibbo-allowed $D^0 \rightarrow K^-\pi^+$ decays can be a significant background to the suppressed process $D^0 \rightarrow K^-K^+$, we have studied the charm particle lifetimes using a variety of Čerenkov cuts. The Čerenkov particle identification cuts used in FOCUS are based on likelihood ratios between the various stable particle identification hypotheses. These likelihoods are computed for a given track from the observed firing response (on or off) of all cells within the track’s ($\beta = 1$) Čerenkov cone for each of our three, multicell threshold Čerenkov counters.¹⁸ The probability that a given track will fire a given cell is computed using Poisson statistics based on the predicted number of photoelectrons striking the cell’s phototube under each particle identification hypothesis and an intensity dependent accidental firing rate determined for each of the 300 cells. The product of all firing probabilities for all cells within the three Čerenkov cones produces a χ^2 -like variable called

¹⁷ This primary vertex is found using a candidate driven vertex finder where a primary vertex is found by intersecting (nucleating) tracks about a “seed track” constructed using the secondary vertex and the reconstructed D momentum vector. This vertexing method allows one to find primary vertices with relatively high efficiency even at very low detachment.

¹⁸ The three Čerenkov counters have pion thresholds of 4.5, 8.4, and 17.4 GeV/c.

$W_i \equiv -2 \log(\text{likelihood})$ where i ranges over the electron, pion, kaon, or proton hypotheses.

The mass distributions of Figure 1 illustrate the use of these likelihood-based Čerenkov cuts. Figure 1(a) shows the $D^0 \rightarrow K^- \pi^+$ signal obtained after requiring $W_\pi - W_K > 4$ for the K^- . This Čerenkov cut, which we will call *kaonicity*, implies that the track we are assigning to the kaon has an observed Čerenkov pattern under the kaon hypothesis that is favored over that of the pion hypothesis by a factor of $e^2 = 7.39$. To further reduce backgrounds for the untagged component of this signal, we put an additional cut on the track reconstructed as a kaon that the proton light pattern is not favored over the kaon hypothesis by more than $\Delta W = 3$. We also use a pion consistency cut which requires that no particle hypothesis is favored over the pion hypothesis with a ΔW exceeding 2. Over the momentum spectrum of typical tracks in FOCUS, pions have significantly different Čerenkov response than kaons, and only a small fraction (typically $< 15\%$) have $W_\pi - W_K > 0$. Thus, even a mild cut on the likelihood ratio favoring the kaon hypothesis on the track which is being assigned to the kaon reduces backgrounds to Cabibbo-favored decays such as $D^0 \rightarrow K^- \pi^+$, $K^- \pi^+ \pi^- \pi^+$ and $D^+ \rightarrow K^- \pi^+ \pi^+$ by a factor ≈ 10 .

Figures 1(b) and 1(c) illustrate the use of a tight $W_\pi - W_K$ cut to reduce the $D^0 \rightarrow K^- \pi^+$ reflection background to $D^0 \rightarrow K^- K^+$. The reduction of the $K^- \pi^+$ reflection is evident as ΔW , applied to both tracks, is raised from 1 to 4. The $D^0 \rightarrow K^+ K^-$ signal yield is estimated using a Gaussian signal peak over a background consisting of a 5th-order polynomial to represent general backgrounds along with a $K^- \pi^+$ reflection line shape taken directly from Monte Carlo but scaled by a fit parameter to best match the data. We vary the detachment cuts, Čerenkov cuts, and the background parameterization in order to assess the systematics due to both charm reflection and other backgrounds.

Because the $D^0 \rightarrow K^+ K^-$ signals have significant reflection backgrounds due to misidentified $D^0 \rightarrow K^- \pi^+$ decays, we use a modified version of the mass sideband subtraction fitting technique used in our preceeding experiment [4]. The basic E687 lifetime fitting technique fits the reduced proper time histogram for $D^0 \rightarrow K^+ K^-$ or $D^0 \rightarrow K^- \pi^+$ signal region events to a corrected exponential distribution added to the reduced proper time histogram taken for combinations falling in either the high or low mass sideband. Because this technique assumes that the events in symmetrically placed mass sidebands have the same lifetime evolution as events in the background within the signal region, it must be modified in light of the $K^- \pi^+$ misidentification reflection shown in Figure 1 which only populates the upper sideband. In order to accommodate this reflection, we use a *subtracted* upper sideband time histogram where we subtract the expected contribution from the $D^0 \rightarrow K^- \pi^+$ reflection from the raw upper sideband, reduced proper time histogram. The overall nor-

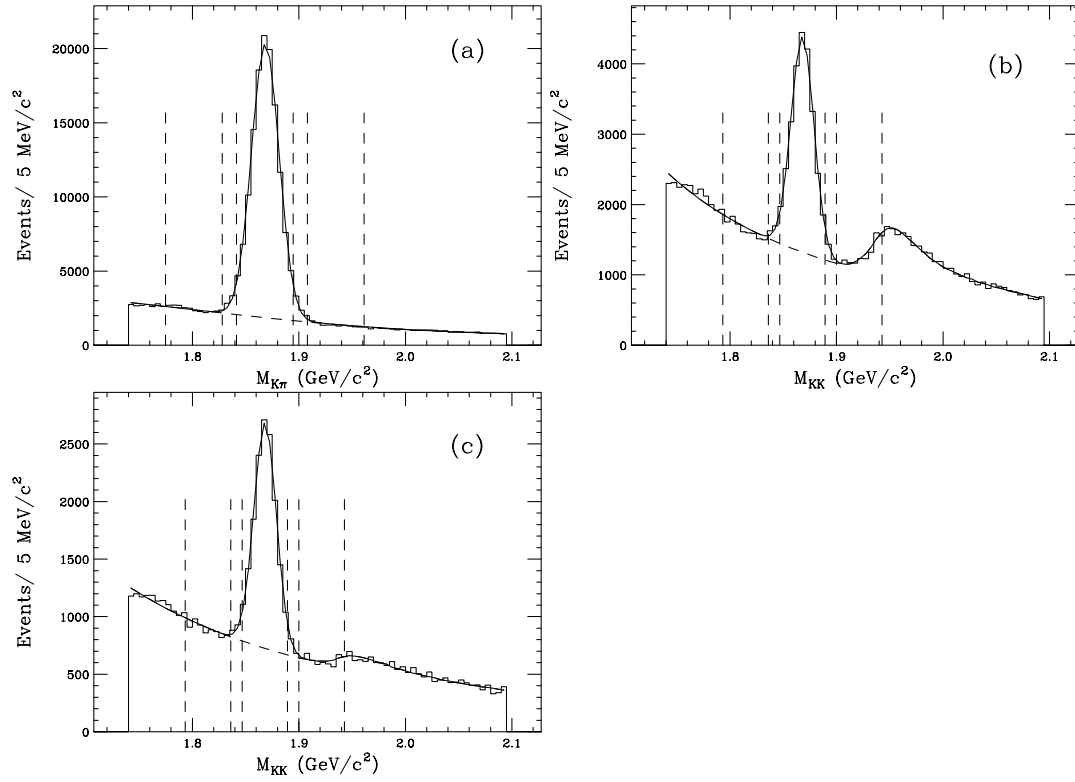


Fig. 1. (a) Signal for $D^0 \rightarrow K^-\pi^+$ with a detachment cut of $\ell/\sigma > 5$ and $W_\pi - W_K > 4$. The yield is 119 738 $K^-\pi^+$ signal events. Signals for $D^0 \rightarrow K^+K^-$ with a detachment cut of $\ell/\sigma > 5$. The reflection in the background at higher masses is due to contamination from misidentified $D^0 \rightarrow K^-\pi^+$. (b) Requiring $W_\pi - W_K > 1$, we obtain a yield of 16 532 K^+K^- signal events. (c) Requiring $W_\pi - W_K > 4$, we obtain a yield of 10 331 K^+K^- signal events. The vertical dashed lines indicate the signal and side-band regions used for the lifetime and y_{CP} fits.

malization of the reflection contribution is computed using information from the fits to the $D^0 \rightarrow K^+K^-$ mass spectrum illustrated in Figure 1. The reduced proper time shape is computed using the lifetime of the $D^0 \rightarrow K^-\pi^+$. This lifetime is taken from a joint fit of the $D^0 \rightarrow K^+K^-$ and $K^-\pi^+$ reduced proper time distributions where the four fit parameters are (1) lifetime of the $D^0 \rightarrow K^-\pi^+$, (2) the y_{CP} parameter which relates the $D^0 \rightarrow K^+K^-$ lifetime to the $D^0 \rightarrow K^-\pi^+$ lifetime, (3) the background level under the $K^-\pi^+$ signal, and (4) the background level under the K^-K^+ signal.¹⁹

The reduced proper time contributions for the $D^0 \rightarrow K^-\pi^+$, $D^0 \rightarrow K^-K^+$ and misidentified $D^0 \rightarrow K^-\pi^+$ reflection are of the form $f(t') \exp(-t'/\tau)$ where $f(t')$ represents efficiency and absorption corrections to a pure expo-

¹⁹ The exponential signal contributions follow from the total number of events in each signal region minus the background level fit parameter.

ponential decay with lifetime τ .²⁰ A separate $f(t')$ correction factor is used for each of the three exponential contributions. Figure 2 shows the efficiency and absorption corrections obtained from our Monte Carlo for both decay modes in 200 fs bins of reduced proper time.²¹ The $f(t')$ function is obtained by dividing the simulated reconstructed charm yield in each reduced proper time bin by the input decay exponential integrated over the bin. Figure 2 shows that the Monte Carlo corrections are typically less than 5% for both decay modes and the corrections for K^+K^- are statistically consistent with those for $K^-\pi^+$. Sources of potential $f(t')$ variation include a minor relative depletion at low t' since the charm secondaries must lie within the fiducial area of the downstream microstrips, a depletion at large t' for charm candidates decaying within and downstream of the microstrip detector, and a slight depletion at low t' since the upstream charm daughters need to travel through more material before exiting a target segment for the $\approx 30\%$ of events whose secondary vertex lies in target material. The charm daughter absorption effect is partially compensated when one considers absorption of the charm particle itself which tends to favor low t' for those events produced within the target material.²² Because FOCUS uses a segmented target consisting of four 6.75 mm thick BeO sections, each separated by 10 mm, many decays occur in air. The charm absorption is minimized in this configuration creating only minor corrections to the fitted lifetimes.²³ Except for the $\approx 24\%$ difference between the absorption cross section for kaons and pions in the momentum range relevant to D^0 's reconstructed in FOCUS, the very small absorption correction will be common to both decay modes considered here [5].

The background level for both the $D^0 \rightarrow K^-\pi^+$ and $D^0 \rightarrow K^+K^-$ are parameters in the lifetime fit. We have employed two ways of determining these

²⁰ The use of a multiplicative “efficiency” correction, rather than an integral over a resolution function is justified since our reduced proper time resolution is less than 1/10 th of the D^0 lifetime. Because of the somewhat large (200 fs) bin widths, we actually integrate the exponential over the domain of the bin in computing the signal contribution rather than just evaluating the exponential at the bin center.

²¹ Our Monte Carlo simulation includes the Pythia model for photon-gluon fusion and incorporates a complete simulation of all detector systems, with all known multiple scattering and particle absorption effects. We have confirmed that it accurately reproduces the momentum and P_\perp distribution for D mesons and the multiplicity of the primary vertex. The Monte Carlo was run with $20\times$ the statistics of the experiment.

²² We assume that the charm absorption cross section is 1/2 of the cross section for neutrons. Uncertainty in the charm cross section should cancel when the charm decay lifetimes are compared.

²³ For example, computing the $f(t')$ correction using a Monte Carlo where the absorption cross sections for charm secondaries have been scaled by a factor of 60% relative to their known values, causes the lifetimes for the K^+K^- and $K^-\pi^+$ to decrease by about 1.2 fs.

parameters which are used to normalize the background contribution to the reduced proper time histogram in the signal region. The first method determines the background levels by finding a level which best fits the time evolution in the signal region. The second method combines information from the lifetime evolution with additional information from the fits to the mass distribution such as those shown in Figure 1. We accomplish this by adding additional likelihood terms which tend to “tie” the total background level to that deduced from the mass fit.²⁴ The incorporation of information from the mass fit tends to reduce errors by 15–20% compared to the fits where the background level is determined from the time evolution alone.

Figure 3 shows the t' evolution for the $D^0 \rightarrow K^- \pi^+$ and $D^0 \rightarrow K^- K^+$ along with the predicted number from the lifetime fit. The confidence level for these fits are 2% and 55%, for the $K^- \pi^+$ and $K^+ K^-$, respectively. From these fits we obtain a lifetime asymmetry of:

$$y_{\text{CP}} = \frac{\Gamma(\text{CP even}) - \Gamma(\text{CP odd})}{\Gamma(\text{CP even}) + \Gamma(\text{CP odd})} = (3.42 \pm 1.39 \pm 0.74)\%$$

and a $D^0 \rightarrow K^- \pi^+$ lifetime of

$$\tau(D^0 \rightarrow K^- \pi^+) = 409.2 \pm 1.3 \text{ fs (systematics not evaluated)}.$$

Using our value for the fitted lifetime asymmetry, we compute $\tau(D^0 \rightarrow K^- K^+) = 395.7 \pm 5.5 \text{ fs}$ (systematics not evaluated). We have used a variety of approaches to assess our systematic errors. We assessed systematics by studying the consistency of four samples split according to momentum and primary vertex location for a variety of detachment and Čerenkov cuts.

The systematic errors were estimated by studying the variation of the fitted lifetime estimates as the analysis cuts and fitting technique are varied and by looking at the internal consistency of subsamples of the data.²⁵ Because

²⁴ Specifically for the $D^0 \rightarrow K^- \pi^+$ we add the log likelihood of a Poisson distribution which ties the $D^0 \rightarrow K^- \pi^+$ level to half of the sum of the number of candidates in the upper and lower sideband. For the $D^0 \rightarrow K^+ K^-$ we add a χ^2 -like likelihood penalty term which ties the background level to the integral of the polynomial used to represent the background under the $D^0 \rightarrow K^+ K^-$ peak in the signal region.

²⁵ These include comparing the results for a high momentum sample versus a low momentum sample, the sample originating in the upstream two targets versus downstream two targets, the tagged versus inclusive portion of the signal and the use of different width mass sidebands.

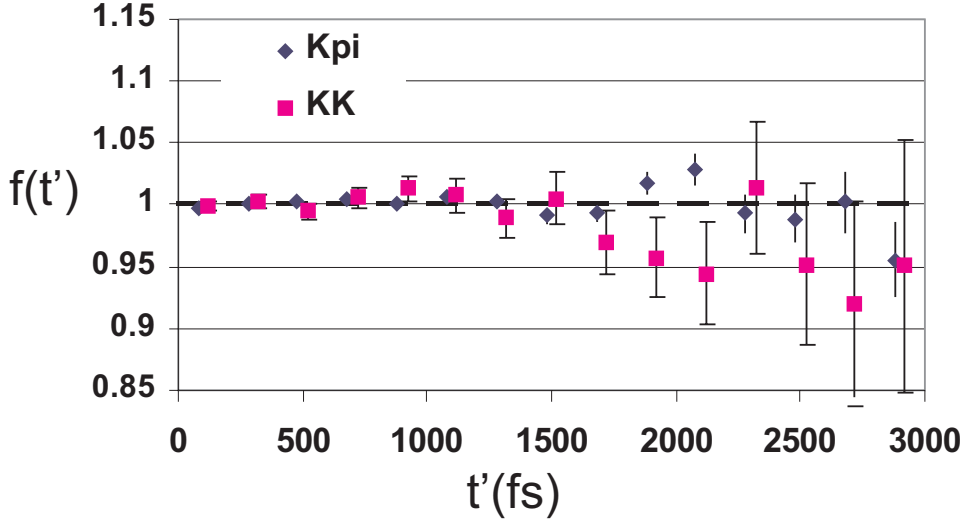


Fig. 2. Monte Carlo correction factors for $D^0 \rightarrow K^-\pi^+$ and K^-K^+ for $\ell/\sigma > 5$ and $W_\pi - W_K > 4$. We have offset the K^-K^+ points slightly for clarity and have given them “flats” on their error bars. Monte Carlo corrections are rather slight with these cuts and the corrections for $D^0 \rightarrow K^-\pi^+$ are the same within errors as those for $D^0 \rightarrow K^+K^-$.

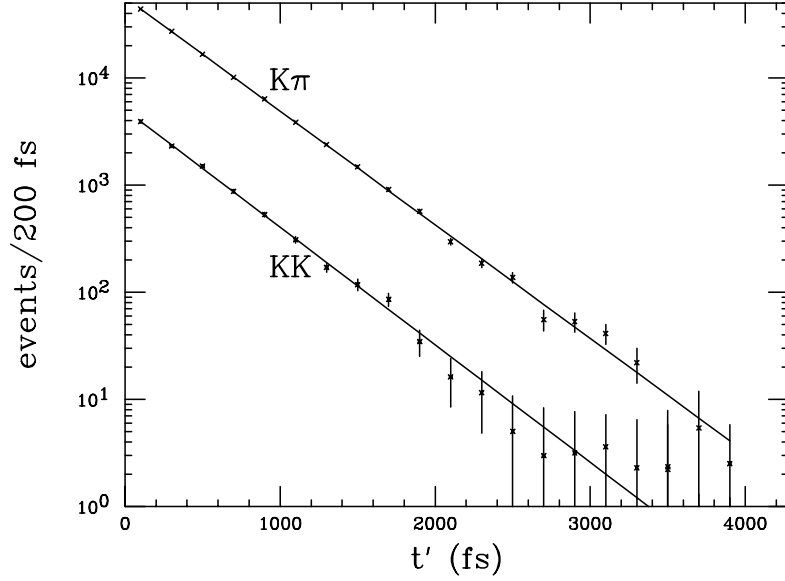


Fig. 3. Signal versus reduced proper time for $D^0 \rightarrow K^-\pi^+$ and K^-K^+ requiring $W_\pi - W_K > 4$ and $\ell/\sigma > 5$. The fit is over 20 bins of 200 fs bin width. The data is background subtracted and includes the (very small) Monte Carlo correction.

the Monte Carlo corrections shown in the $f(t')$ plots (Figure 2) are consistent between the $D^0 \rightarrow K^-\pi^+$ and K^+K^- sample, one expects the dominant systematic error on y_{CP} to come from potential differences in the background under the K^+K^- peak. By varying the minimum ℓ/σ cut from 5 to 9 for the case of $K^-\pi^+$ and K^+K^- , we significantly change the relative background level

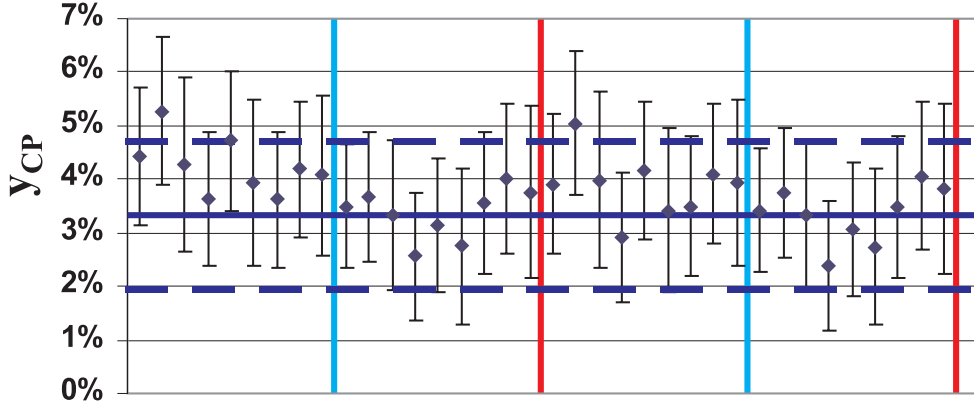


Fig. 4. Stability of the y_{CP} results for 9 sets of clean-up cuts and 4 different fit variants. The set of 9 fit variants consists 3 different kaonicity cuts ($\Delta W_K > 1, 2, 4$), each with three different detachment cuts $\ell/\sigma > 5, 7, 9$. The first 18 values use a 15 bin fit; the last 18 values use a 20 bin fit, where the bin size remains fixed at 200 fs. The 1st and 3rd set of 9 values obtain the background level entirely through the time fit. The 2nd and 4th set use the background level which incorporates additional information from the mass fits shown in Figure 1. The RMS spread in these values is 0.63 % which is considerably smaller than our statistical errors.

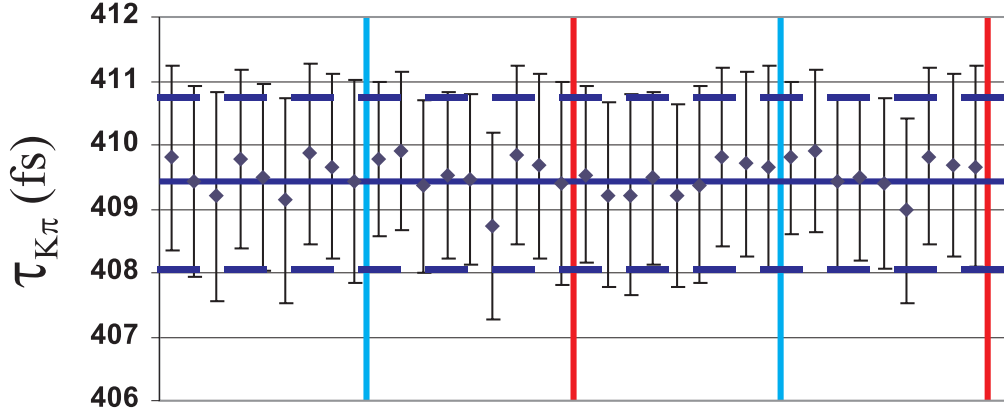


Fig. 5. Stability of the $\tau(K^-\pi^+)$ results for 9 sets of clean-up cuts and 4 different fit variants. The 36 estimates are plotted according to the convention of Figure 4. The RMS spread in these values is 0.28 fs which is considerably smaller than our statistical errors.

by eliminating non-charm backgrounds.²⁶ Changing the Čerenkov log likeli-

²⁶ Defining the signal-to-noise as the ratio of the signal height to background height at the location of the Gaussian signal peak, the fits used to measure the lifetimes have signal-to-noise ratios which range from 8.9 to 19.3 for the $K^-\pi^+$, from 2.3 to 5.7 for the K^-K^+ .

hood ratio cuts from $\Delta W = 1$ to 4 significantly changes the level of charm reflection contamination (as evidenced by Figure 1), and reduces contamination from combinatoric background. Figure 4 demonstrates the stability of the y_{CP} results for 9 sets of cleanup cuts and 4 different fit variants. The 9 cleanup cut variants considered were 3 different kaonicity cuts ($\Delta W_K > 1, 2, 4$), each with three different detachment cuts $\ell/\sigma > 5, 7, 9$.²⁷ Figure 4 also summarizes the results on y_{CP} for four variants of the fitting technique. These fitting variants include varying the lifetime range and the method used to obtain the background level. We show the fitted $D^0 \rightarrow K^-\pi^+$ lifetime for each of the 9 cut variants and 4 fit variants in Figure 5. Our quoted systematic error was evaluated by first calculating the shifts in y_{CP} for three different detachment cuts, three different kaonicity cuts, two different background level options, and three different lifetime fit ranges. These shifts were then combined in a conservative manner by adding them in quadrature to obtain the quoted systematic error.

We have presented new measurements of the lifetime ratio between a CP even final state, $D^0 \rightarrow K^-K^+$ and a CP mixed decay, $D^0 \rightarrow K^-\pi^+$. Our analysis techniques have been designed to minimize the relative systematic errors between these samples, rather than to obtain the best statistical error on the D^0 lifetime under the assumption of a pure exponential decay.²⁸ E791 [2] measures $\Delta\Gamma = 2(\Gamma_{KK} - \Gamma_{K\pi}) = 0.04 \pm 0.14 \pm 0.05 \text{ ps}^{-1}$. Combining this and their measurements of the KK and $K\pi$ lifetimes, we obtain a value of $y_{\text{CP}} = (0.8 \pm 2.9 \pm 1.0)\%$ which is consistent with our measured value of $y_{\text{CP}} = (3.42 \pm 1.39 \pm 0.74)\%$.

A more recent result exists from the CLEO Collaboration. CLEO searches for mixing effects by studying the possible interference of mixing with direct doubly-Cabibbo-suppressed decays in the time evolution of $D^{*+} \rightarrow \pi^+(K^+\pi^-)$ decays [6]. They report a 95 % confidence level range on a variable they call y' of $-5.8\% < y' < 1\%$. If the level of CP violation in charm decays is negligible, the CLEO y' variable is a rotational transformation of the y_{CP} variable reported here and a variable which depends on the CP eigenstate mass difference with the angle of rotation being due to a strong phase shift. Theoretical estimates on the size of this angle differ significantly [7] making a precise comparison of our result with the CLEO result impossible at the present time.

²⁷ Each set of 9 points is ordered as $(\Delta W_K > 1, \ell/\sigma > 5)$, $(\Delta W_K > 2, \ell/\sigma > 5)$, $(\Delta W_K > 4, \ell/\sigma > 5)$, $(\Delta W_K > 1, \ell/\sigma > 7)$, $(\Delta W_K > 2, \ell/\sigma > 7)$, $(\Delta W_K > 4, \ell/\sigma > 7)$, $(\Delta W_K > 1, \ell/\sigma > 9)$, $(\Delta W_K > 2, \ell/\sigma > 9)$, and $(\Delta W_K > 4, \ell/\sigma > 9)$.

²⁸ For example, inclusion of the $D^0 \rightarrow K^-\pi^+\pi^-\pi^+$ decay mode would essentially double our statistics for the D^0 lifetime. In addition, there are systematic error sources such as the overall distance scale error which affects our absolute lifetime but not the lifetime ratio which is the principle result reported here.

Because of our high statistics, the error on y_{CP} reported here can be reliably interpreted as a Gaussian error for the purposes of combining with other measurements.²⁹ This measurement represents the most precise direct measurement of the neutral D meson CP eigenstate lifetime difference.

We wish to acknowledge the assistance of the staffs of Fermi National Accelerator Laboratory, the INFN of Italy, and the physics departments of the collaborating institutions. This research was supported in part by the U. S. National Science Foundation, the U. S. Department of Energy, the Italian Istituto Nazionale di Fisica Nucleare and Ministero dell'Università e della Ricerca Scientifica e Tecnologica, the Brazilian Conselho Nacional de Desenvolvimento Científico e Tecnológico, CONACyT-México, the Korean Ministry of Education, and the Korean Science and Engineering Foundation.

²⁹ The χ^2 versus τ in a $\pm 1 \sigma$ domain about the fit minimum is well fit by a parabola.

References

- [1] Harry Nelson, UCSB HEP 99-08 (Aug. 1999), e-Print Archive: hep-ex/0001060 and references therein; E. Golowich, Proceedings of the Conference on B Physics and CP Violation, Honolulu, HI (March 1997) and references therein; A.A. Petrov, Phys. Rev. D56,1685 (1997); E. Golowich and A.A. Petrov, Phys. Lett. B427 (1998) 172; J.F. Donoghue, E. Golowich, B.R. Holstein and J. Trampetic, Phys. Rev. D33 (1986) 179; T. Ohl *et al.*, Nucl. Phys. B403 (1993) 605.
- [2] E791 Collab., E. M. Aitala *et al.*, Phys. Rev. Lett. 83 (1999) 32.
- [3] E687 Collab., P. L. Frabetti *et al.*, Nucl. Instrum. Methods Phys. A 320 (1992) 519.
- [4] See for example E687 Collab., P. L. Frabetti *et al.* Phys. Rev. Lett. 70 (1993) 1755 ; Phys. Rev. Lett. 71 (1993) 827 ; Phys. Lett. B323 (1994) 459.
- [5] Particle Data Group, C. Caso *et al.*, Eur. Phys. J. C3 (1998) 1.
- [6] CLEO Collab., R. Godang *et al.*, CLNS-99-1659, Dec 1999, submitted to Phys. Rev. Lett. e-Print Archive: hep-ex/0001060.
- [7] A. F. Falk, Y. Nir, A. A. Petrov, JHEP 9912:019,1999.